INELASTIC SEISMIC RESPONSE OF BRIDGE DRILLED-SHAFT RC PILE/COLUMNS

By A. M. Budek,[1] M. J. N. Priestley,[2] and G. Benzoni,[3] Member, ASCE

ABSTRACT: An analytical model based on a Winkler beam is used to represent the lateral force response of a reinforced concrete (RC) pile in cohesionless soil. An inelastic finite-element analysis was performed on the structure, using as the pile constitutive model the section moment-curvature relationship based on confined stress-strain relationships for the concrete. Parameters varied were pile head restraint (free and fixed head), height of pile head above grade level, and soil stiffness. Linear, bilinear, and hyperbolic soil models were examined. The analysis showed that shear would be significantly underpredicted by an elastic analysis, as inelastic behavior moved the point of maximum moment in the pile shaft closer to the surface, thus reducing the shear span. Maximum moment depth in the pile shaft and plastic hinge length were also shown to be strongly dependent on soil stiffness, and in the case of fixed-head piles, on abovegrade height of the superstructure. Linear soil models were shown to be adequate for most cases of pile/column design.

INTRODUCTION

Cast-in-drilled-hole (CIDH) reinforced concrete (RC) piles have seen recent widespread use as a cost-effective method of transferring superstructure loads into some depth of soil. They may provide support for a foundation or footing or may have a column section of similar diameter appended at grade level via a construction joint (the latter forming a pile/column). Construction of CIDH piles begins with the augur-drilling of the shaft to the desired depth. A cage of reinforcing steel is placed in the hole, which is then filled to grade level. The superstructure (footing, foundation, or column) is then joined to the pile.

While the design of piled footings favors forcing plasticity into the superstructure, with the piles remaining elastic, pile/columns should be designed with ductile performance in mind. In the case of a single pile/column, formation of a plastic hinge in the pile shaft is the only mechanism by which ductile performance can be attained. A pile/column bent will first form hinges at the column/cap beam joint, but the full flexural capacity of the system may only be obtained through the formation of a secondary, subgrade hinge.

Fig. 1 shows the moment patterns that result from the lateral loading of a pile (or pile/column). In the case of a free-head pile/column, the plastic hinge that controls inelastic response will form in the shaft below grade level. The controlling hinge in a fixed-head pile will develop at the pile-cap connection; attainment of the full inelastic potential of this hinge will generally result in the formation of a second, subgrade hinge. (Note that the bent in Fig. 1 represents a fixed-head pile/column; for a footing or foundation substructure, $H = 0$).

The aim of the research considered herein was to perform nonlinear parametric analyses on both free- and fixed-head pile/columns in cohensionless soil, varying soil stiffness and superstructure height. In the case of fixed-head pile/columns, it was assumed that the pile spacing would be greater than 3D (as would be the case in a typical bridge bent), and therefore shadowing effects were not considered. Two nonlinear soil models were also examined. A quasistatic stepwise-monotonic approach was taken for loading; dynamic amplification effects are generally not a concern in bridge structures, and dynamic soil-structure interaction has minimal impact in cohesionless soils (Priestley et al. 1996).

REVIEW OF PREVIOUS RESEARCH AND DESIGN METHODS

Most of the analytical work on piles that has been done to date has assumed linear-elastic pile response; this is largely a development of the design philosophy, mentioned above, that locates hinges in the superstructure and assumes elastic pile response.

The elastic-continuum model has been, and remains, a powerful tool in the dynamic analysis of piles; it also can model pile groups. However, as the name implies, it is a method limited to elastic analysis of pile and soil.

Early attempts at lateral analysis of the pile-soil system (Howe 1955; Matlock and Reese 1960; Bowles 1968) used the finite-difference method to produce a set of nondimensional curves for design use. A designer could enter the curves for given lateral loading, pile characteristics, and soil properties and obtain estimation of head deflection and maximum bending moment. These attempts necessarily used only selected and generalized variations of soil characteristics with depth. Reese (1977) extended the early work to incorporate nonlinear soil characteristics in the form of p–y curves (p = pressure, y = displacement), which predict the relationship of soil modulus (which corresponds to the stiffness of the soil spring) to the displacement of the pile. In general, p–y curves change with

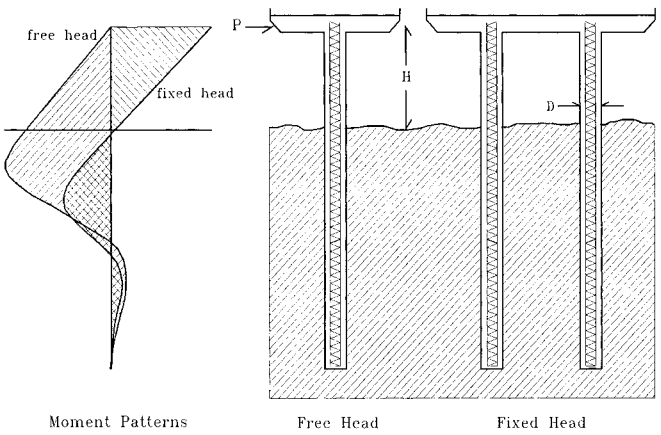

FIG. 1. Moment Patterns in Free- and Fixed-Head CIDH Piles

[1]Postgrad. Res. Engr., Dept. of Struct. Engrg., Univ. of California at San Diego, La Jolla, CA 92093-0085.

[2]Prof. of Struct. Engrg., Univ. of California at San Diego, La Jolla, CA.

[3]Res. Engr., Dept. of Struct. Engrg., Univ. of California at San Diego, La Jolla, CA.

Note. Associate Editor: Brad Cross. Discussion open until September 1, 2000. To extend the closing date one month, a written request must be filed with the ASCE Manager of Journals. The manuscript for this paper was submitted for review and possible publication on March 10, 1999. This paper is part of the ***Journal of Structural Engineering***, Vol. 126, No. 4, April, 2000. ©ASCE, ISSN 0733-9445/00/0004-0510–0517/ $8.00 + $.50 per page. Paper No. 20434.

depth, and one must use a $p-y$ curve with depth-dependent stiffness.

While the finite-difference method was well suited for use with limited computing power (it produces a stiffness matrix $N \times N$, in which N is the number of nodes in the structure), it has some disadvantages. Unless layering of elements is used, it requires that all elements be of the same length. The main area of interest in a free-head pile, for example, is that from ground level to about 10 pile diameters subgrade; nodes should be closely spaced there, but the small variations in rotation and displacement in other areas mean that elements could be made larger with little loss of accuracy. Using finite difference, this is possible only with layering, and so the initial advantage of an $N \times N$ stiffness matrix (that of a manageable number of computations) is lost if the nodal spacing is set for good accuracy in the critical area.

The drastic increase in low-cost computational power beginning in the 1970s has brought the use of the finite-element method (FEM) to the fore. FEM uses a larger stiffness matrix, incorporating both displacement and rotation, and has the added advantage of being able to process elements of various sizes. One may therefore have as fine a mesh as one might wish in the critical region, while giving up little in speed of analysis. Another advantage of FEM is ease of modeling different boundary conditions (i.e., for a fixed-head pile, a no-rotation end condition can be easily specified). Nonlinear properties for soil and pile may be incorporated in the analysis comparatively simply.

One of the major aspects of ductile performance in piles (and, for that matter, in all reinforced concrete structures) is predictable curvature demand. A study by Banerjee, Stanton, and Hawkins (1987) examined the theoretical bending behavior of single piles subjected to severe ground motion at three sites (Seattle, Tacoma, and San Francisco). The analysis consisted of two steps: first, a free-field analysis for relevant soil profiles to model ground motions in the absence of a structure, which was then used as, second, an input for a modeled soil-structure interaction. The free-field analysis used the University of California at Berkeley-developed computer code SHAKE; this program was used to calculate the motion of bedrock required to cause a given surface motion for a given soil profile. For the Washington State sites, the April 13, 1949, record from the Olympia Highway Test Laboratory was used, giving 20 s duration with a maximum ground acceleration of $0.28g$. The San Francisco example used a scaled record of the 1952 Kern County earthquake, scaled to a bedrock depth of 87 m, yielding a peak ground acceleration of $0.45g$ and a predominant period of 0.42 s. (This corresponds to a magnitude 8.25 earthquake with an epicentral distance of 16 km.) The second part of the analysis, the soil-structure interaction, was attacked with the aid of FLUSH, a computer program that iteratively solved the complex harmonic equilibrium equations for the system at each frequency of excitation and then performed a time-history analysis of the soil-pile interaction. The results of this study tend to confirm engineering intuition: First, that larger curvatures could be expected in relatively softer soils; second, that large curvature demands could occur at soil layer interfaces of significantly different soil moduli; third, that the pile-pile cap interface would be the critical region insofar as curvature demand was concerned; and finally, that increasing pile size decreased curvature demand (though it should be noted that increasing pile diameter usually results in reduced curvature capacity). However, the conclusions must be viewed with some caution as they were based on elastic pile properties; they could differ when softening in the region of the plastic hinge is considered.

The currently accepted design procedure for piles can be summarized as follows (*Caltrans* 1990):

1. Determination of an equivalent column length (that is, length to fixity for an equivalent cantilever column of the same stiffness to produce the same displacements under lateral load) from design charts.
2. Equivalent-cantilever analysis to determine expected displacements and rotations at column top.
3. Detailed analysis of individual pile/columns using a special-purpose code, such as the California Department of Transportation (Caltrans)' ''PILE'' (*Caltrans* 1990) to determine bending moments and depth to maximum moment.

The pile shaft length is designed so that ''long'' pile behavior results. That is, the pile is sufficiently long so that further increases in pile length would not reduce lateral displacements at yield. An adaptation of the Caltrans (1990) graph relating soil conditions, pile diameter, and depth to effective fixity is shown in Fig. 2.

A relationship between N, the standard penetration index, and K, the subgrade reaction modulus, is given by

$$K = 530N \text{ kN/m}^3 \tag{1}$$

This comes from work by Scott (1981), modifying earlier conclusions by Terzaghi and Peck (1948) and Terzaghi (1955). This relationship is calibrated for a pile of diameter $D = 1.83$ m. It should be noted that (1) is a good predictor of cohesionless soil strength; it should not be applied to cohesive soils.

Although this approach is relatively sophisticated, it does not consider inelastic response of soil and pile. Fig. 2 indicates that depth to fixity is independent of column height, which is questionable, since shear corresponding to flexural strength reduces with height, reducing lateral reactions in the soil and thus mobilizing a lesser depth of soil. Finally, there is no rational basis for determining plastic displacement, and hence displacement ductility capacity, since this depends on plastic hinge length, which has not been defined for pile shafts.

Early analysis by Terzaghi (1955) suggested that soil stiffness is independent of pile diameter, though this model tended to underpredict deflections of small-diameter piles. Later work by Ling (1988) shows that a much better relationship between predicted and observed deflection is obtained by assuming a linear relationship between soil stiffness and pile diameter; this stiffness assumption was adopted for this study.

Displacement ductility capacity of pile shaft designs, if calculated at all, has been generally based on an assumed plastic hinge length in the shaft of $l_p = D$ (where D = pile diameter),

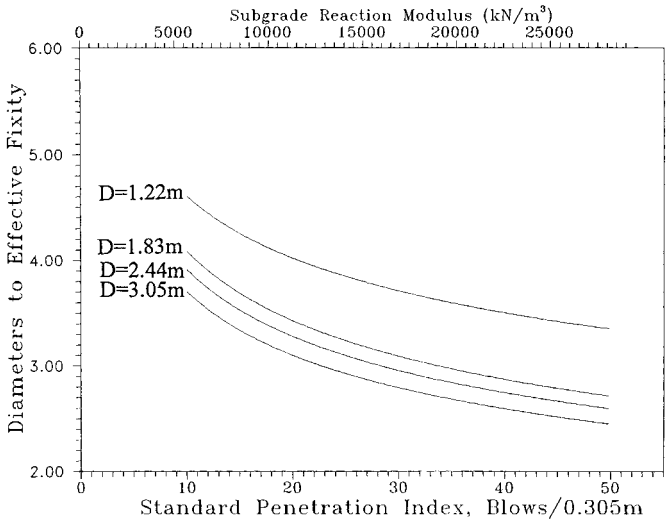

FIG. 2. Depth to Fixity Used by Caltrans (1990) for Piles in Sand

based largely on intuition, without any particular supporting theory or experimental evidence.

For plastic hinges forming against supporting members such as footings or cap beams, theoretical and experimental studies have led to the development of the following equation for plastic hinge length (Priestley et al. 1996)

$$l_p = 0.08L + 0.022 f_y d_{bl} \quad (2)$$

where L is the distance from the critical section to the point of contraflexure, f_y is the yield strength in MPa, and d_{bl} is the longitudinal bar diameter. The first term in (2) represents the spread of plasticity resulting from variation in curvature with distance from the critical section, and assumes a linear variation in moment with distance. The second term represents the increase in effective plastic hinge length associated with strain penetration into the supporting member.

It is apparent that (2) is inappropriate for plastic hinges forming in pile shafts since (1) Inelastic curvature can be expected to spread both above and below the critical section; (b) the slope of the moment profile at the section of maximum moment is zero, invalidating the assumption of a linear decrease in moment with distance from the critical section; and (c) there should be no strain-penetration effect, since at the critical section there should be no significant slip of tension reinforcement past the section (which results in the strain penetration effect for a fixed-base plastic hinge) because of the approximate symmetry of the moment profile about the critical section.

METHOD OF ANALYSIS

The analyses described in the present work were carried out to provide a better definition of the ductility capacity and to specifically identify the parameters influencing equivalent plastic hinge length, depth to equivalent fixity for displacement, and depth to position of maximum moment. A soil with stiffness increasing linearly with depth (typical for a granular soil) was assumed.

The basic model for the analysis was a Winkler beam (a beam on a bed of springs). The FEM representation is illustrated in Fig. 3; note that each subgrade node is associated with a soil spring, whose specific stiffness is defined by the subgrade reaction modulus of the soil (K; kN/m^3) multiplied by the depth of the node z_i, multiplied by the node's tributary length L_i. Thus, for an individual soil spring at node i

$$k_i = z_i \times L_i \times K \quad (3)$$

The lateral load is applied at the pile head, and the pile end is fixed against rotation and lateral displacement. The load is stepwise-monotonic. The depth of the pile end was chosen to allow ''pile'' (not ''pole'') behavior, in which the end displacements are less than 0.001 times the head displacement. Element lengths ranged from $D/12$ (in the plastic hinge region adjacent to the cap beam in fixed-head pile/columns) to $1.33D$ (at the pile foot).

The pile section considered in this analysis was a typical design for a pile/column, with a diameter of 1.83 m and a cover of 50.4 mm. Longitudinal reinforcement was provided by 36 #14 Grade 60 bars (D43, 415 MPa nominal), giving a longitudinal steel ratio of 0.02; transverse reinforcement was in the form of #6 Grade 60 spiral (D19, 415 MPa nominal) pitched at 110 mm, resulting in a volumetric transverse reinforcement ratio of 0.006.

Concrete strength of 27.6 MPa and an axial load of $0.1 f'_c A_g$ were assumed. Probable yield strength of rebar was assumed to be 455 Mpa, 10% above the nominal grade value. Moment-curvature properties [calculated using the Mander model (Mander et al. 1988) for confined concrete] for the section are shown in Fig. 4. The moment-curvature representation is discretized; section stiffness EI at any point on the curve is equal to the slope of that segment.

The value of the abovegrade height H was varied from 2 to 10 pile diameters D. Two pile head restraint conditions were examined: free head (no restraint) and fixity of the head against rotation.

Soil models were parameterized over a range $3{,}200 \leq K \leq 48{,}000$ kN/m^3. From (1), this represents a standard penetration index range of 10 to 88 blows/ft (0.305 m). Three soil models were examined: a linear-elastic relationship for soil spring stiffness; a bilinear model in which the stiffness of an individual soil spring was assumed to drop to one-fourth of its initial value after 25.4 mm lateral displacement; and a hyperbolic model developed by Carter (1984) that allows a finite-element representation of soil defined by $p-y$ curves. Representative soil spring lateral force and stiffness versus displacement are shown in Figs. 5 and 6.

The hyperbolic model is based upon the assumption that, initially, the small-strain subgrade reaction modulus (which is approximately four times greater than the ''global'' value used in the linear and bilinear analyses) will more accurately reflect soil properties. As can be seen in Fig. 6, this implies a much greater initial system stiffness. At larger displacements, nearparity with the bilinear model is reached.

The analysis was begun by calculating the lateral force and displacement that would result in a moment at which first yield

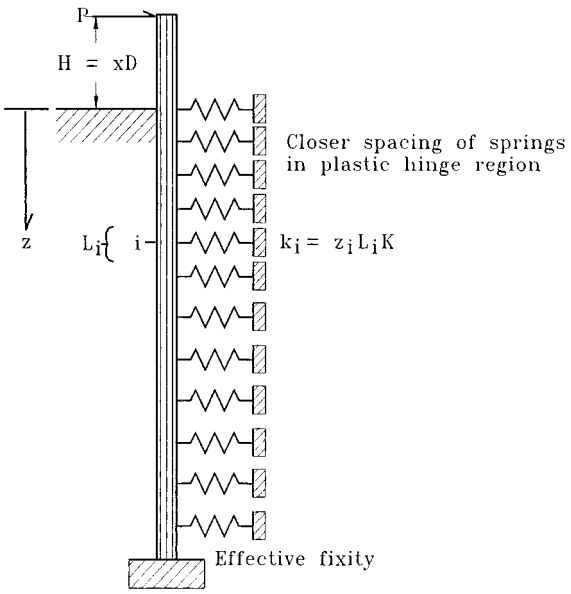

FIG. 3. Winkler Beam Model of Soil-Pile System (D-Pile Diameter)

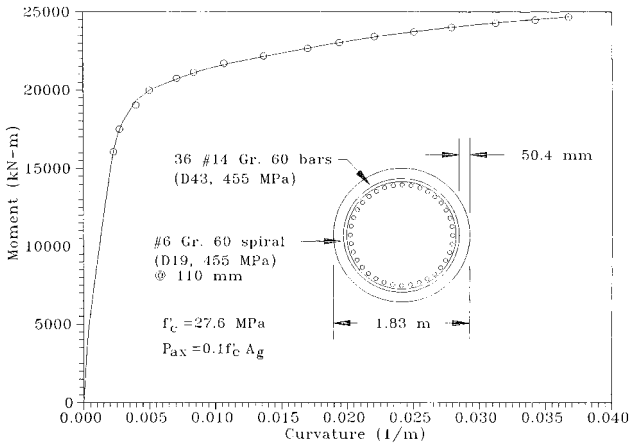

FIG. 4. CIDH Pile Section and Theoretical Moment-Curvature Properties

of the tension steel would occur; the initial pile stiffness used was the cracked-section stiffness. The average moment at each element was then checked; any element with an average moment within 3% of yield was assumed to have yielded, and its stiffness was then reduced to correspond to the slope (tangent stiffness) of the applicable portion of the moment-curvature curve. The use of nonlinear soil models required that the load be ''stepped'' to yield, to more correctly model soil behavior.

Analysis of fixed-head piles incorporated the effect of strain penetration into the cap [see (2)]. This has the effect of softening the connection (as opposed to the neglecting of strain penetration) and was modeled by reducing the stiffness of the topmost element at the pile head through division by a factor s_p:

$$s_p = \frac{\text{element length} + \text{strain penetration length}}{\text{element length}}$$

The next force target was the next (discrete) point on the moment-curvature curve; a lateral force was applied to achieve this moment as the maximum moment in the structure, and then, as before, elements whose average moment was in the inelastic range had their stiffnesses reduced. This process was continued until the maximum moment achieved was that which corresponded to the maximum allowable concrete strain predicted by the moment-curvature analysis.

To extend the range of applicability of the analysis results, quantities compared to the variation of K are plotted against a nondimensional system stiffness, given by

$$KD^6/D^*EI_{eff} \tag{4}$$

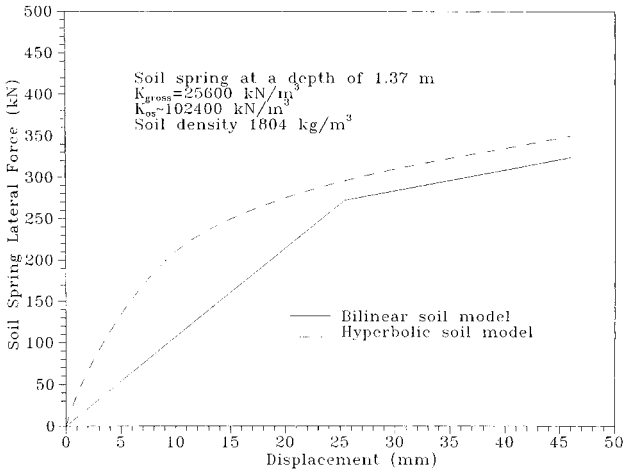

FIG. 5. Soil Spring Lateral Force versus Lateral Displacement

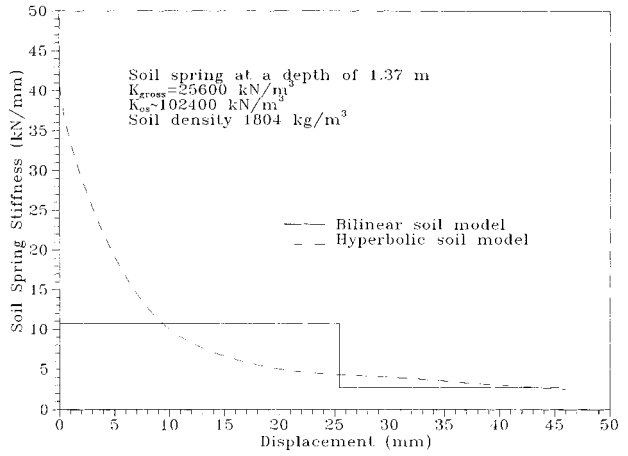

FIG. 6. Soil Spring Stiffness versus Lateral Displacement

in which K = subgrade reaction modulus (kN/m^3); D = pile diameter (m); D^* = 1.83 m; and EI_{eff} = effective cracked-section stiffness. The validity of this expression for characterizing nondimensional system stiffness was verified by analysis of pile/columns of different diameter (Budek et al. 1995).

RESULTS

Free-Head Pile/Columns in Elastic Soil

Fig. 7 shows a family of moment patterns at ultimate displacement capacity over a range of soil stiffnesses (3,200 $\leq$ $K \leq$ 32,000 kN/m^3) for a free-head pile/column with $H = 5D$ in an elastic soil. Of particular interest is the manner in which the point of maximum moment moves toward grade level with increasing soil stiffness; also, emplacement in soft soils will require the pile shaft to carry a relatively higher moment to a greater depth than in stiffer soils.

The relationship of the depth of the plastic hinge to the parameters examined is shown in Fig. 8. The greatest variation is seen at low values of height H and subgrade reaction modulus K; shear forces that must be transferred from the pile to the soil are greatest at low values of H, and softer soils require greater mobilization. The hinge depth (in which the shear demand is implicit) is therefore affected to the greatest degree under these conditions.

Fig. 9 shows moment patterns (at K = 25,600 kN/m^3 for a free-head pile with $H = 5D$) at ultimate moment for an in-

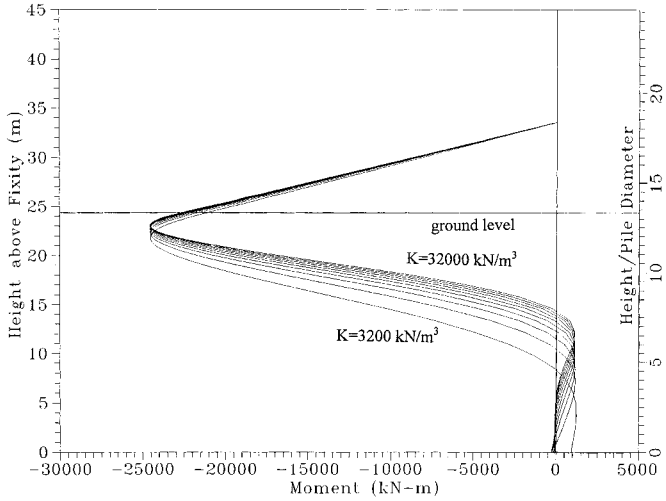

FIG. 7. Moment Patterns at Ultimate Displacement Capacity in Free-Head Pile/Column in Elastic Soil ($H = 5D$, 3,200 $\leq K \leq$ 32,000 kN/m^3)

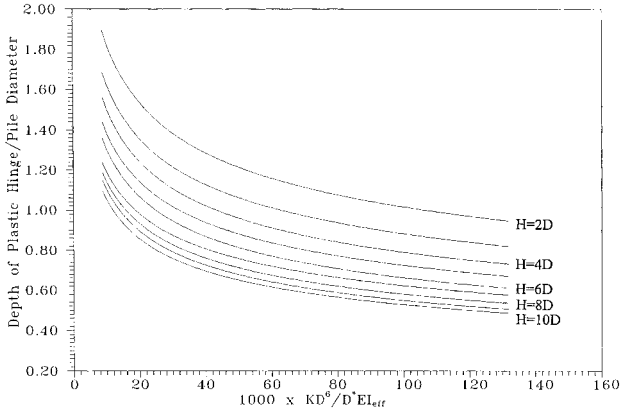

FIG. 8. Depth of Plastic Hinge versus Nondimensional System Stiffness, Free-Head Pile/Column ($2D \leq H \leq 10D$, 3,200 $\leq K \leq$ 48,000 kN/m^3)

elastic pile analysis, at ultimate moment for a purely elastic pile analysis, and at yield. What is immediately apparent is the manner in which the depth of the point of maximum moment is greater for the elastic case. The reason for this is that the softening of the structure after yield requires the mobilization of a smaller depth of soil.

The ratio of the depth of the point of maximum moment based on elastic pile behavior to the depth of the plastic hinge in an inelastic pile analysis is examined in Fig. 10. The results are very consistent, with no variation due to changing soil stiffness (the ''range'' of values was caused by discretization of the structure). The median value is ≈1.44 over the full range of $3{,}200 \leq K \leq 48{,}000$ kN/m^3. Thus, the depth to the position of the in-ground hinge would reasonably be interpreted for a pile with moderate ductility demand from an elastic analysis, reducing the predicted depth by dividing by 1.44.

Fig. 11 shows force-displacement response for the pile-soil system representing the examined ranges of above-grade height and subgrade modulus. The trends to higher system stiffness and shear force and to lower overall displacement (albeit with little change in displacement ductility capacity) with increasing soil stiffness are evident. The response is nearly bilinear in its aspect and suggests the following characterization of the ratio of second-slope stiffness to initial stiffness:

$$r = \left(\frac{K_p}{K_e}\right) = 0.15 - 0.006\,\frac{H}{D} - (0.02)^{10(D/H)} \tag{5}$$

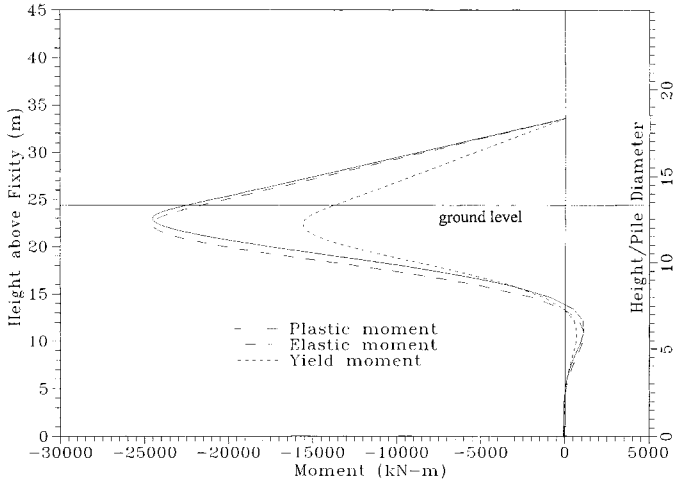

FIG. 9. Moment Patterns at Ultimate (Inelastic and Elastic Analyses) and at Yield in Free-Head Pile/Column in Elastic Soil (K = 25,600 kN/m^3; $H = 5D$)

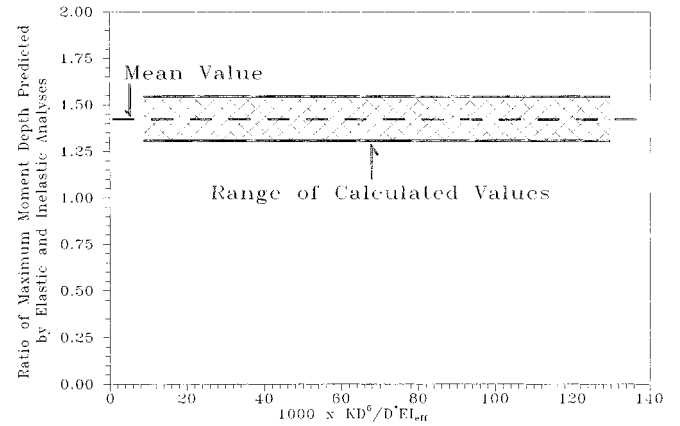

FIG. 10. Ratio of Maximum Moment Depth for Free-Head Pile/Column Predicted by Elastic and Inelastic Analyses in Elastic Soil ($3{,}200 \leq K \leq 48{,}000$ kN/m^3)

in which K_p = second-slope stiffness; K_e = initial (elastic) stiffness; H = abovegrade height; and D = pile diameter.

The plastic hinge length is shown for the parameters examined in Fig. 12. It is calculated by

$$l_p = \frac{\Theta_p}{\phi_p} \tag{6}$$

in which Θ_p = plastic rotation; and ϕ_p = plastic curvature. The plastic rotation was measured as the plastic displacement of the pile head divided by the distance from the pile head (or, in the case of fixed-head piles, the point of inflection) to the point of initial yielding in the pile shaft. Dependence of l_p on both soil stiffness and abovegrade height is nearly linear and suggests the following (conservative) linearization:

$$l_p = D + 0.06H \tag{7}$$

in which D = pile/column diameter; and H = abovegrade height (in multiples of D).

This equation is approximately correct for nondimensional system stiffness of $KD^6/D^*E_{eff} = 0.10$. For more flexible soils the plastic hinge length may be considerable longer, as shown by Fig. 12.

Displacement ductility capacity was found to be relatively insensitive to either abovegrade height or soil stiffness. For the level of transverse reinforcement assumed in this analysis, a displacement ductility capacity of 3.3 was found. This was essentially independent of the stiffness or the height ratio.

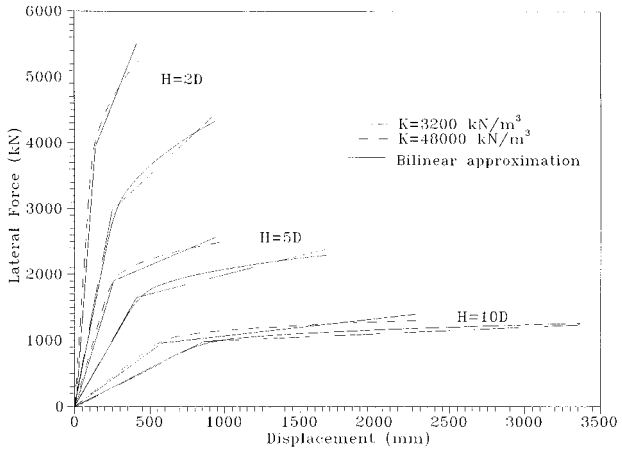

FIG. 11. Force-Displacement Response, Free-Head Pile/Column in Elastic Soil Compared with Bilinear Approximation from Eq. (5) ($H = 2D$, $5D$, and $10D$; K = 3,200 and 48,000 kN/m^3)

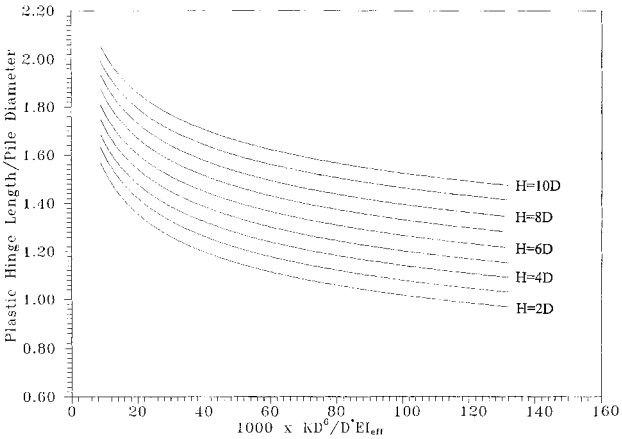

FIG. 12. Plastic Hinge Length versus Nondimensional System Stiffness for Free-Head Pile/Column in Elastic Soil ($2D \leq H \leq 10D$, $3{,}200 \leq K \leq 48{,}000$ kN/m^3)

However, since the ultimate curvature will depend on section details, axial load ratio, and lateral reinforcement ratio, the ductility capacity (and hence force reduction factor for design) should be checked for pile details differing from those of Fig. 4.

Abovegrade shear is relatively insensitive to soil stiffness, being dictated by the moment capacity of the pile. Shear below the plastic hinge in the pile shaft increases with soil stiffness, as shown in Fig. 13, but this would not be expected to be an actual factor on pile performance, as any tendency to shear deformations in this part of the pile shaft would be adequately resisted by the surrounding soil.

In Fig. 14 a comparison is shown of shear versus height as H is varied from $2D$ to $10D$ at a midrange value of K. An interesting effect is apparent here: The peak shear force below the in-ground plastic hinge is essentially independent of the column height above grade, and hence of the ground-level shear force, which varies greatly between the $2D$ and $10D$ cases. Thus the in-ground shear appears to depend solely on the pile moment capacity and the characteristic soil stiffness.

Fixed-Head Pile/Column in Elastic Soil

Moment patterns at ultimate displacement capacity are shown in Fig. 15 for a fixed-head pile/column with $H = 5D$, and $3{,}200 \leq K \leq 32{,}000$ kN/m^3. As in the free-head case, the point of maximum moment moves toward the surface of the soil as the soil stiffness increases. The depth of the point of maximum moment for a fixed-head pile/column follows a pattern similar to that of a free-head pile/column, in that the greatest variation is seen at low values of height H and subgrade reaction modulus K. The higher shear demand imposed by pile/columns of smaller values of H requires the mobilization of a greater depth of soil, and softer soils must be mobilized to a greater depth.

Fig. 16 shows a comparison of ultimate inelastic, ultimate elastic, and yield moment pattern for a fixed-head pile/column ($H = 5D$; $K = 25{,}600$ kN/m^3). It may clearly be seen that development of the full inelastic potential of the pile-cap connection implies the development of much larger subgrade moments (and possible hinging) than would be indicated by an elastic-pile analysis to the same value of maximum moment. Again, the depth of the maximum subgrade moment in the elastic case is lower than in the elastic analysis.

The ratio of maximum moment depths predicted by elastic and inelastic analyses bracket a median value of 1.25. This is somewhat less than the value of 1.44 for a free-head pile/column, shown in Fig. 10. In the fixed-head case, the subgrade hinge is not fully developed by the point at which the hinge at the cap reaches its capacity; the pile shaft is therefore stiffer and requires a somewhat greater depth of mobilization of soil.

Fig. 17 shows the force-displacement response for a fixed-head pile/column ($H = 5D$; $3{,}200 \leq K \leq 32{,}000$ kN/m^3). As in the free-head case, a bilinear approximation is suggested:

$$r \left(= \frac{K_p}{K_e} \right) = 0.26 - 0.16 \frac{H}{D} \tag{8}$$

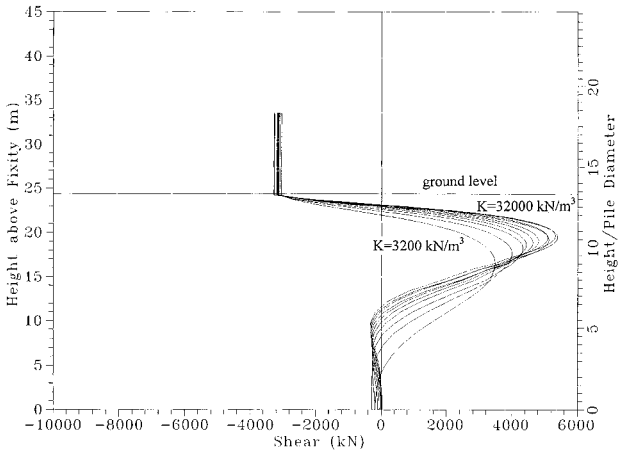

FIG. 13. Shear versus Height, Free-Head Pile/Column in Elastic Soil ($H = 5D$, $3{,}200 \leq K \leq 32{,}000$ kN/m^3)

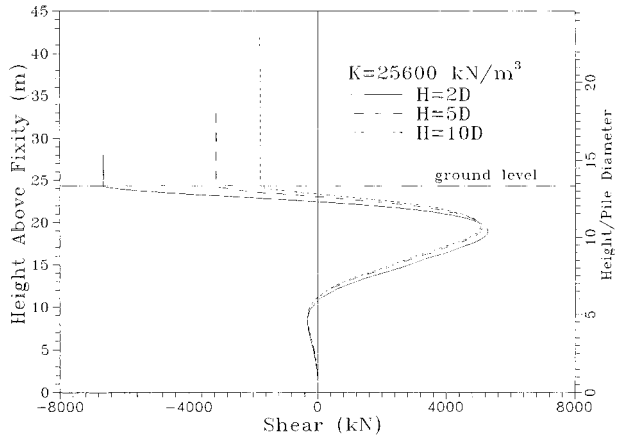

FIG. 14. Shear versus Height, Comparison of Free-Head Pile/Columns of $H = 2D$, $5D$, and $10D$ in Elastic Soil at $K = 25{,}600$ kN/m^3

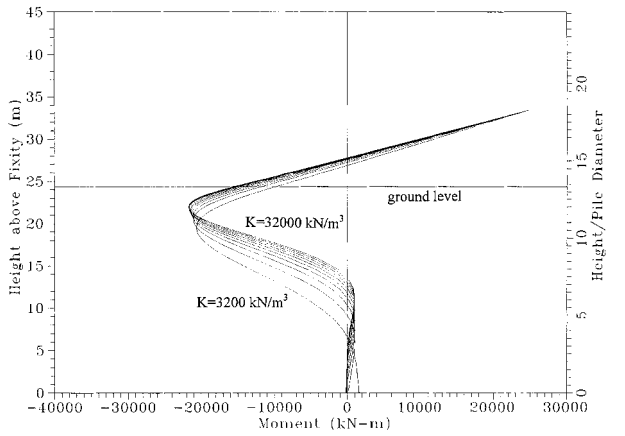

FIG. 15. Moment Patterns at Ultimate Displacement Capacity in Fixed-Head Pile/Column in Elastic Soil ($H = 5D$, $3{,}200 \leq K \leq 32{,}000$ kN/m^3)

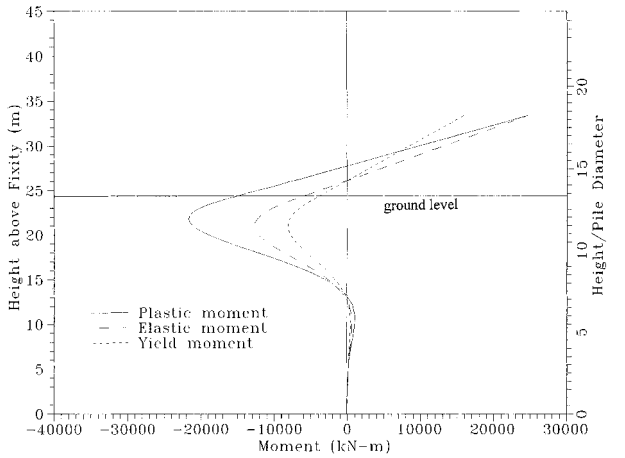

FIG. 16. Moment Patterns at Ultimate (Inelastic and Elastic Analyses) and at Yield in Fixed-Head Pile/Column in Elastic Soil ($K = 25{,}600$ kN/m^3; $H = 5D$)

in which K_p = second-slope stiffness; K_e = initial (elastic) stiffness; H = abovegrade height; and D = pile/column diameter.

The plastic hinge length (for the hinge forming at the pile-cap connection; this hinge controls inelastic response) is insensitive to the soil stiffness and shows a linear variation with height from a minimum of $0.5D$ (at $H = 2D$) to a maximum at $H = 10D$ of $0.85D$.

The displacement ductility capacity of the fixed-head pile/column is more dependent on soil stiffness than is the free-head case; variation with respect to abovegrade height is weak. The displacement ductility capacity may thus be expressed for $3{,}200 \leq K \leq 48{,}000$ kN/m^3:

$$\mu_\Delta = 2.9 + \frac{K}{133{,}333 \text{ kN/m}^3} + 0.05\,\frac{H}{D} \tag{9}$$

for $K > 48{,}000$ kN/m^3

$$\mu_\Delta = 3.4 + 0.05\,\frac{H}{D} \tag{10}$$

Abovegrade shear is, as in the free-head case, not very sensitive to soil stiffness, particularly as the value of K increases into middle and higher ranges. Shear below the subgrade hinge is strongly affected by soil stiffness, but as mentioned above, this is not a practical concern.

Equivalent Beam Depth to Fixity

Figs. 18 and 19 show the depth to fixity for an equivalent beam for both the free-head and fixed-head cases. Both are strongly dependent on soil stiffness; the equivalent cantilever response of the free-head case is only weakly dependent on abovegrade height. Abovegrade height is a more significant factor for the fixed-head equivalent beam. It is to be recalled that the Caltrans equivalent beam approach (Fig. 2) does not take abovegrade height into consideration; this may be considered acceptable for a free-head pile/column, but is not satisfactory in the fixed-head case, particularly at low values of H.

Nonlinear Soil Models

Fig. 20 compares the force-displacement response produced by linear, bilinear, and hyperbolic soil models for a free-head pile/column over a range of $2D \leq H \leq 10D$ at $K = 25{,}600$ kN/m^3. The largest impact caused by soil nonlinearity occurs at low values of H; more soil is mobilized, and thus the role it plays in the structural response is proportionally greater as H decreases. The hyperbolic model is initially stiffer than either the linear or bilinear models, being based, as it is, on the small-strain subgrade reaction modulus of the soil. The hyperbolic model also predicts lower displacements, though the overall level of displacement ductility capacity is similar. As would be expected, the depth of the plastic hinge is greatest for the bilinear model; there is little difference in plastic hinge depth between the linear and hyperbolic models. Hyperbolic

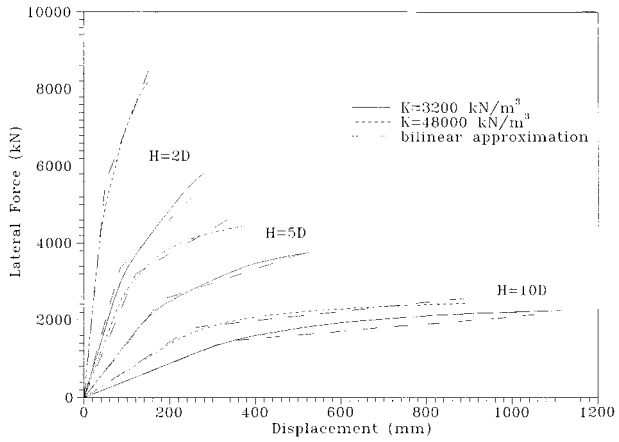

FIG. 17. Force-Displacement Response, Fixed-Head Pile/Column in Elastic Soil, Compared with Bilinear Approximation from Eq. (8) ($H = 2D$, $5D$, and $10D$; $K = 3{,}200$ and $48{,}000$ kN/m^3)

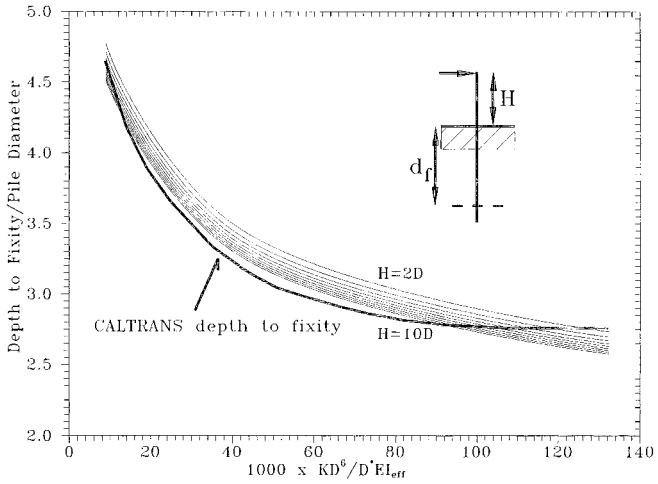

FIG. 18. Equivalent Depth to Fixity, Free-Head Pile in Elastic Soil

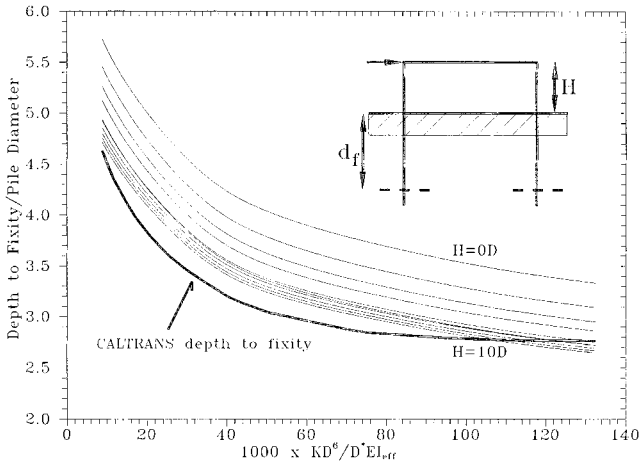

FIG. 19. Equivalent Depth to Fixity, Fixed-Head Pile in Elastic Soil

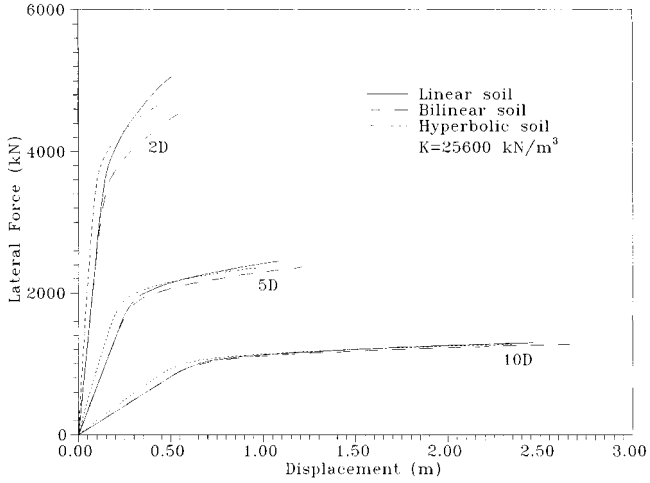

FIG. 20. Force-Deflection Response for Free-Head Pile/Columns in Linear, Bilinear, and Hyperbolic Soils

soil also predicts a sharper drop in moment below the plastic hinge (i.e., the distance from the pile head to the point of inflection is least), which implies higher shear in this region; as mentioned previously, this is not a practical concern. It is questionable to which point the high initial stiffness shown by the hyperbolic model is valid for seismic response; hysteretic behavior of the soil would imply a loss of stiffness.

CONCLUSIONS

Free-Head Pile/Columns

1. A displacement ductility capacity of 3.3 was found for free-head pile/columns at the level of transverse reinforcement found in this analysis; this value was only weakly dependent on soil stiffness of abovegrade height. However, since the ultimate curvature capacity of pile/columns depends on section properties, axial load, and transverse reinforcement level, ductility capacity should be checked and force-reduction factors used in design altered accordingly.
2. A bilinear force-displacement response, with a significant second-slope stiffness, may be assumed. The second-slope stiffness is higher for piles than for equivalent columns because, as plasticity develops, the point of maximum subgrade moment migrates toward the surface, thus reducing the effective shear span.
3. As the structure softens after yield, moments are redistributed up the shaft, and the point of maximum moment (i.e., the subgrade hinge) migrates toward the surface. Thus, depth to plastic hinge may be taken as 0.7 times the depth to maximum moment found through an elastic analysis.
4. Because the lateral resistance provided by the soil serves to spread rotations in the pile shaft over a longer span, the plastic hinge length was found to be significantly greater than the commonly assumed value of one pile diameter D; indeed, for the parameters investigated, this was found to be a lower bound.
5. Because of the migration of the plastic hinge toward the surface in the inelastic range (which reduces the shear span), maximum expected shear above the subgrade hinge should be taken as 1.3 times that found from an elastic-pile analysis to ultimate moment.

Fixed-Head Piles

1. For piles configured as those examined in this study, a displacement ductility capacity in excess of 2.9 was found for soft soils; this increased with increasing soil stiffness. The influence of abovegrade height was weak.
2. The migration of the plastic hinge toward the surface resulted in a significant second-slope stiffness and suggests a bilinear force-displacement response.
3. Plastic hinge length for the controlling hinge at the pile-cap connection is independent of soil stiffness and linearly increased with abovegrade height. The commonly assumed plastic hinge length of $0.5D$ was found to be a lower bound over the range of parameters examined in this study.
4. Maximum expected shear above the point of maximum subgrade moment should be taken as at least 1.3 times that found from an elastic-pile analysis to ultimate moment because of the reduced shear span resulting from the upward migration of the plastic hinge.
5. Because the full flexural capacity of the pile-cap connection may require the formation of a second, subgrade hinge, pile shaft design should take into account the potential for subgrade plastic hinge formation, with appropriate detailing.

Nonlinear Soil Models

1. Use of a linear-elastic soil model was found to be adequate for $H \leq 5D$ and $K \leq 25{,}600$ kN/m^3. Use of a bilinear soil model may be warranted for low values of H and/or K.
2. Soil nonlinearities that increase the depth of the plastic hinge may result in higher system ductilities.
3. The high initial stiffness of the hyperbolic soil model may be of questionable validity for seismic response.

ACKNOWLEDGMENTS

This study was carried out with the support of the California Department of Transportation.

APPENDIX. REFERENCES

Banerjee, S., Stanton, J. F., and Hawkins, N. M. (1987). ''Seismic performance of precast concrete bridge piles.'' *J. Struct. Engrg.*, ASCE, 113(2), 381–396.

Bowles, J. E. (1968). *Foundation analysis and design*., 1st Ed., McGraw-Hill, New York.

Budek, A., Priestley, M. J. N., and Benzoni, G. M. (1995). ''An analytical study of the inelastic seismic response of reinforced concrete pile-columns in cohesionless soil.'' *Rep. No. SSRP-95/13*, Div. of Struct. Engrg., Dept. of Appl. Mech. and Engrg. Sci., University of California, San Diego, La Jolla, Calif.

Caltrans Bridge Design Specifications/Seismic Design References. (1990). Caltrans, Sacramento, Calif.

Carter, D. P. (1984). ''A nonlinear soil model for predicting lateral pile response.'' *Rep. No. 359*, Dept. of Civ. Engrg., University of Auckland, New Zealand.

Howe, R. J. (1955). ''A numerical method for predicting the behavior of laterally loaded piling.'' *Publ. No. 412*, Exploration and Production Res. Div., Shell Oil Co., Houston.

Ling, L. F. (1988). ''Back analysis of lateral load tests on piles,'' ME thesis, Dept. of Civ. Engrg., University of Auckland, New Zealand.

Mander, J. B., Priestley, M. J. N., and Park, R. (1988). ''Observed stress-strain behavior of confined concrete.'' *J. Struct. Engrg.*, ASCE, 114(8), 1827–1849.

Matlock, H., and Reese, L. C. (1960). ''Generalized solutions for laterally loaded piles.'' *J. Soil Mech. and Found Div.*, ASCE, 86(5), 63–91.

Priestley, M. J. N., Seible, F., and Calvi, G. (1996). *Seismic design and retrofit of bridges*. Wiley, New York.

Reese, L. C. (1977). ''Laterally loaded piles—Program documentation.'' *J. Geotech. Engrg. Div.*, ASCE, 103(4), 287–305.

Scott, R. F. (1981). *Foundation analysis*. Prentice-Hall, Engelwood Cliffs, N.J.

Terzaghi, K. (1955). ''Evaluation of the coefficients of subgrade reaction.'' *Géotechnique*, London, 5(4), 297.

Terzaghi, K., and Peck, R. B. (1948). *Soil mechanics in practice*. Wiley, New York.